APPLIED AND ENVIRONMENTAL MICROBIOLOGY, Jan. 2011, p. 657–668 Vol. 77, No. 2
0099-2240/11/$12.00 doi:10.1128/AEM.01806-10

Domain Organization and Evolution of Multifunctional Autoprocessing Repeats-in-Toxin (MARTX) Toxin in *Vibrio vulnificus*▽†

Francisco J. Roig,[1] Fernando González-Candelas,[2,3] and Carmen Amaro[1]*

Departamento de Microbiología, Facultad de Biología, Universidad de Valencia, Valencia, Spain[1]; Unidad Mixta Genómica y Salud Centro Superior de Investigación en Salud Pública-Universidad de Valencia/Instituto Cavanilles de Biodiversidad y Biología Evolutiva, Valencia, Spain[2]; and CIBER de Epidemiología y Salud Pública, Valencia, Spain[3]

Received 30 July 2010/Accepted 2 November 2010

The objective of this study was to analyze multifunctional autoprocessing repeats-in-toxin (MARTX) toxin domain organization within the aquatic species *Vibrio vulnificus* as well as to study the evolution of the *rtxA1* gene. The species is subdivided into three biotypes that differ in host range and geographical distribution. We have found three different types (I, II, and III) of *V. vulnificus* MARTX ($MARTX_{Vv}$) toxins with common domains (an autocatalytic cysteine protease domain [CPD], an α/β-hydrolase domain, and a domain resembling that of the LifA protein of *Escherichia coli* O127:H6 E2348/69 [Efa/LifA]) and specific domains (a Rho-GTPase inactivation domain [RID], a domain of unknown function [DUF],a domain resembling that of the *rtxA* protein of *Photorhabdus asymbiotica* [$rtxA_{PA}$], and an actin cross-linking domain [ACD]). Biotype 1 isolates harbor $MARTX_{Vv}$ toxin types I and II, biotype 2 isolates carry $MARTX_{Vv}$ toxin type III, and biotype 3 isolates have $MARTX_{Vv}$ toxin type II. The analyzed biotype 2 isolates harbor two identical copies of *rtxA1*, one chromosomal and the other plasmidic. The evolutionary history of the gene demonstrates that $MARTX_{Vv}$ toxins are mosaics, comprising pieces with different evolutionary histories, some of which have been acquired by intra- or interspecific horizontal gene transfer. Finally, we have found evidence that the evolutionary history of the *rtxA1* gene for biotype 2 differs totally from the gene history of biotypes 1 and 3.

Vibrio vulnificus is an "accidental" pathogen, inhabiting brackish water ecosystems in temperate and tropical regions (22). The species has been subdivided into three biotypes on the basis of genetic, phenotypic, and host range differences (4, 35). Biotypes 1 and 2 are distributed worldwide while biotype 3 is geographically restricted to Israel (1, 4, 11, 35). Three O serovars have been described in biotype 2 (serovar A, serovar E, and serovar I), and one has been identified in biotype 3 (serovar O) while biotype 1 has not been fully serotyped (2, 5, 11).

The three biotypes of *V. vulnificus* can cause disease in humans after ingestion of contaminated seafood or immersion of an open wound in brackish waters (22). In healthy people, the ingestion of *V. vulnificus* leads to vomiting and diarrhea while external exposure produces wound infection or severe ulcerations; however, in immunocompromised people, particularly those with chronic liver disease, the pathogen can invade the bloodstream and cause septicemia, leading to death in almost 50% of the cases (22). Interestingly, biotype 2 can also infect fish (mainly eels) and shrimps and cause death by hemorrhagic septicemia, a disease called warm-water vibriosis (35). Human isolates of biotype 2 belong to the most virulent fish serovar, serovar E (1).

Several studies have been performed with biotype 1 isolates to elucidate the genetic basis of *V. vulnificus* virulence for humans. These isolates produce a wide range of putative virulence factors, among which is a repeats-in-toxin (RTX) toxin, which belongs to the subfamily of multifunctional autoprocessing RTX (*V. vulnificus* MARTX [$MARTX_{Vv}$]toxin, or RtxA1) toxins. *rtxA1* mutants are less virulent for mice and have lower cytotoxicity for different cell lines (17). The *rtxA1* gene is practically identical in the two sequenced isolates of biotype 1 (7, 15) (98.9% and 99.5% nucleotide and amino acid identity, respectively) and codes for a protein of 5,206 amino acids (aa), which shows extensive regions of similarity with the MARTX toxin of *Vibrio cholerae* ($MARTX_{Vc}$ toxin), the most extensively studied MARTX toxin to date (28). Both toxins share the N- and C-terminal repetitive regions, which seem to be common to all MARTX toxins, a Rho-GTPase inactivation domain (RID), an autocatalytic cysteine protease domain (CPD), and an α/β-hydrolase domain. Meanwhile, they differ in that the biotype 1 $MARTX_{Vv}$ ($MARTX_{Vvbt1}$) toxin lacks an actin cross-linking domain (ACD) and presents three additional putative domains, DUF3 (domain of unknown function), Mcf (a domain similar to an Mcf toxin of *Photorhabdus luminescens*), and PMT C1/C2 (a domain similar to a portion of the *Pasteurella mitogenic* toxin PMT) (27).

The genetic basis underlying fish virulence is related to a recently described plasmid of 68 to 70 kb (18). This plasmid codes for resistance to the innate immune system of fishes and is currently under study. The plasmid also carries an *rtxA1* gene, which codes for a toxin that seems to be a hybrid between the $MARTX_{Vvbt1}$ toxin and the $MARTX_{Vc}$ toxin because it lacks the RID domain and presents an ACD domain (18). Interestingly, the chromosome of the only biotype 2 isolate

* Corresponding author. Mailing address: Departamento de Microbiología, Facultad de Biología, Universidad de Valencia, Valencia, Spain. Phone: 34 96 354 31 04. Fax: 34 96 354 45 70. E-mail: carmen.amaro@uv.es.

† Supplemental material for this article may be found at http://aem.asm.org/.

▽ Published ahead of print on 12 November 2010.

TABLE 1. *V. vulnificus* strains used in the study: source, biotype, and country of isolation

Strain(s)	Biotype/serovar[a]	Origin or reference	Country of isolation
ATCC 33816, CECT 5164, CECT 5168, CECT 5169, CECT 529[T][b,c,d]	t1/NT	Human blood	USA
CECT 5166	Bt1/NT	Wound infection	USA
CECT 5165	Bt1/NT	Seawater	USA
E4, JE	Bt1/NT	Seafood	USA
MLT364, MLT404, MLT406, MLT362, VV1003, VV352, VV425	Bt1/NT	Environment	USA
V4	Bt1/NT	Human blood	Australia
CS9133	Bt1/NT	Human blood	South Korea
CECT 5167, N87, KH03, YN03	Bt1/NT	Human blood	Japan
L49	Bt1/NT	Brackish water	Japan
YJ106[d]	Bt1/NT	Human blood	Taiwan
CG118	Bt1/NT	Seawater	Taiwan
CG100[d], CG106	Bt1/NT	Oyster	Taiwan
CG110, CG111	Bt1/NT	Seawater	Taiwan
CECT 4867	Bt1/NT	Diseased eel	Sweden
94-9-118	Bt1/NT	Human expectoration	Denmark
94-9-130	Bt1/NT	Water	Denmark
94-9-119[c]	Bt1/NT	Human wound	Denmark
A2, A4, A5, A6, A7, PD-1, PD-3, PD-5, PD-12, PD-2-66, V1	Bt1/NT	Eel tank water	Spain
CECT 4606[d]	Bt1/NT	Healthy eel	Spain
Riu-1[c], Riu-3	Bt1/NT	Seawater	Spain
94385	Bt1/NT	Leg wound	Spain
CECT 4608	Bt1/NT	Eel farm water	Spain
CECT 5768, A13, A21, A22, CECT 5689[d], CECT 5769, A15, A16, A17, A18, CECT 5198, CECT 5343, A10, A11, A14[c,d]	Bt2/SerA	Diseased eel	Spain
4/7/17, 4/7/19, 21B, 22, 26, 27, 21A	Bt2/SerA	Diseased eel	Denmark
CECT 4864, CECT 4999[d], CECT 4605, CECT 4607, CECT 4604[d], CECT 4602, CECT 4603, CECT 4601	Bt2/SerE	Diseased eel	Spain
PD-2-47, PD-2-50, PD-2-51, PD-2-55, PD-2-56, CECT 5763	Bt2/SerE	Eel tank water	Spain
C1, CECT 5762	Bt2/SerE	Healthy eel	Spain
Riu-2[d]	Bt2/SerE	Seawater	Spain
CIP8190	Bt2/SerE	Human blood	France
CECT 4868	Bt2/SerE	Diseased eel	Norway
90-2-11	Bt2/SerE	Diseased eel	Denmark
4-8-112	Bt2/SerE	Human wound	Denmark
94-9-123	Bt2/SerE	Seawater	Denmark
CCUG38521	Bt2/SerE	Human blood	Sweden
Ö122	Bt2/SerE	Diseased eel	Sweden
CECT 4866	Bt2/SerE	Human blood	Australia
CECT 4865	Bt2/SerE	Diseased shrimp	Taiwan
UE516	Bt2/SerE	Diseased eel	Taiwan
CECT 898, CECT 897, CECT 4174[d], CECT 4862	Bt2/SerE	Diseased eel	Japan
95-8-161[c,d], 95-8-162	Bt2/SerI	Diseased eel	Denmark
CECT 4869	Bt2/SerI	Diseased eel	Belgium
95-8-7	Bt2/SerI	Diseased eel	Denmark
95-8-6[d]	Bt2/SerI	Diseased eel	Denmark
97, 162, 11028[c,d], vv12, vv32	Bt3/SerO	Diseased human	Israel
CT218[c,d,e]	Bt2/SerE	18	

[a] Bt, biotype; NT, nontypeable; SerE, serovar E; SerA, serovar A; SerI, serovar I; SerO, serovar O.
[b] Type strain.
[c] Strain used to sequence the whole *rtxA* gene.
[d] Strain used to locate the *rtxA* gene.
[e] Cured derivative biotype 2 isolate.

studied in detail so far also harbors a copy of *rtxA1* although it is as yet unknown whether this copy is similar to the plasmidic or the $MARTX_{Vvbt1}$ toxin one (18). The relevance of both copies for virulence in fishes and mice is currently under study.

Considering the aforementioned results, we hypothesized that the *rtxA1* gene of *V. vulnificus* is a mosaic gene, which varies within and among biotypes because it has acquired, probably through horizontal gene transfer (HGT) and subsequent integration into the original allele, some DNA sequences from different bacterial species. To test this idea, we studied the domain structure of $MARTX_{Vv}$ toxin as well as the evolution of the *rtxA1* gene in *V. vulnificus* using different approaches. First, we sequenced the complete *rtxA1* gene in seven isolates and a 828-bp fragment from the 5′ region of the gene in a collection of 115 strains of different biotypes and serovars (Table 1). Second, we analyzed the mosaic domain organization of the predicted protein by comparing it with the sequences previously published in *V. vulnificus* (strains YJ016, CMCP6, CECT 4999, and CECT 4602), *V. cholerae* (strain N16961), *V. splendidus* (12B01), and *Aeromonas hydrophila* (strain ATCC 7966) (27). The sequences of the MARTX

toxin of *V. cholerae* M66-2, AM19226, N16961, MO10, and O395 as well as of *Listonella anguillarum* M93 (20) were also included although the domain organization of these proteins has not been published previously. Finally, we analyzed the phylogeny of the *rtxA1* gene from whole gene sequences, from the sequences of the selected common fragment, and from each separate domain using the previously published homologous sequences from *V. cholerae*, *V. splendidus*, *A. hydrophila*, and *L. anguillarum* as outgroups.

MATERIALS AND METHODS

Bacterial strains and growth conditions. The *V. vulnificus* strains used in this study are listed in Table 1. Strains were routinely grown in Trypticase soy broth or agar plus 5 g liter^{-1} NaCl (TSB-1 or TSA-1, respectively; Pronadisa, Spain) at 28°C for 24 h. For genomic DNA extraction, bacteria were grown overnight with shaking at 28°C. The strains were maintained both as lyophilized and as frozen stocks at −80°C in marine broth (Difco) plus 20% (vol/vol) glycerol.

DNA extractions. Genomic DNA was extracted according to the mini-prep protocol for genomic DNA extraction (3). Plasmid DNA was extracted following the TENS protocol (36) with the modifications of Roig and Amaro (24).

Location of the *rtxA1* gene. The *rtxA1* gene was located in the chromosome or in the plasmids of the strains CECT 529^T, YJ106, CG100, CECT 4606, CECT 5689, A14, CECT 4999, CECT 4604, Riu-2, CECT 4174, 95-8-161, 95-8-6, 11028, and CT218 (Table 1) by Southern hybridization, essentially as described by Roig and Amaro (24). Briefly, DNA samples were subjected to electrophoresis in 0.7% (wt/vol) agarose gels (molecular grade; Roche) and transferred to the membranes (zeta-probe blotting membrane; Bio-Rad) with a vacuum blotter (model 785; Bio-Rad) following the manufacturer's instructions. The samples were genomic DNA extractions (3) and plasmid extractions (24). As molecular weight markers (MWM) Generuler DNA ladder mix and plasmids of the *E. coli* strain 39R861 were used. Probes of 1,087 nucleotides (nt) were generated from PCR products obtained with primers 2F and 2R (Table 2) labeled with digoxigenin (DIG)-11-dUTP (Roche, Switzerland), and the probes against the MWM were derived from the MWM using a DIG High-Prime kit (Roche, Switzerland. Hybridization was performed using a DIG Easy Hyb Granules kit (Roche, Switzerland), and color was developed with anti-digoxigenin-alkaline phosphatase (AP) Fab fragments together with blocking reagent (Roche, Switzerland), which were used following the manufacturer's instructions.

PCR and DNA sequencing. To sequence the whole *rtxA1* gene in the strains CECT 529^T, 94-9-119, Riu-1, A14, 95-8-161, 11028, and CT218 and the common fragment (an 828-bp fragment from the 5′ region of the gene obtained with the primers 12F and 12R) in the *V. vulnificus* collection of strains, PCRs were performed using the primers listed in Table 2. These primers were designed from the published genome sequences of two human biotype 1 strains (YJ016 and CMCP6) (7, 15) and of the plasmids of two biotype 2 strains (CECT 4999 and CECT 4602) (18). Reaction mixtures for PCRs (120 μl) contained 0.48 mM forward and reverse primer, 2.5 units of *Taq* DNA polymerase (5 U/μl GoTaq; Promega), 18 μl of 5× *Taq* reaction buffer (Gotaq Green; Promega), 1.3 mM $MgCl_2$, 0.75 mM deoxynucleoside triphosphate (dNTP) mix (Promega), and 1 μl of DNA. PCRs were performed in a Techne thermocycler (TC-412). The reaction started with 10 min of denaturation at 94°C and was followed by 45 cycles of 40 s of denaturation at 94°C, 45 s of annealing at 52°C, and 90 s of extension at 72°C. An additional extension at 72°C for 10 min completed the reaction. A negative (no template DNA) and a positive (purified DNA of positive isolates) control were included in each PCR batch. Amplified products were separated by electrophoresis at 100 V for 30 min in a 2% (wt/vol) agarose (Low EEO; Pronadisa) gel with Tris-acetate-EDTA (TAE) buffer (Real, Spain) and were visualized by staining with ethidium bromide.

Highly conserved regions, repetitive regions, and protein domain analysis. The highly conserved terminal regions of the *rtxA1* genes sequenced in this work were identified by alignment of the amino acid sequences of the following: $MARTX_{Vc}$ toxin of strains M66-2, AM19226, MO10, O395, and N16961 (YP_002810174.1, YP_002175744.1, ZP_05237921.1, NC_009457.1, NC_002505.1, respectively); MARTX toxin of *L. anguillarum* ($MARTX_{La}$) of isolate M93 (EU_155486.1); MARTX toxin of *V. splendidus* ($MARTX_{Vs}$) of strain 12B01 (ZP_00989505.1); and $MARTX_{Vv}$ toxin of YJ016, CMCP6, CECT 4999, and CECT 4602 (YP_001393222.1, YP_001393065.1, NP_937086.1, and NP_762440.1, respectively) using the program AlignX from Invitrogen. Repetitive sequences were identified by searching the consensus sequences in the alignments using the MEGA program as sequence editor (33) and the AlignX (Invitrogen) and Expasy programs (12). Finally, the domains were determined as described by Satchell (27) by direct alignment by using InterProScan Sequence Search, Superfamily, Psi-BLAST, and SBase Web programs.

Phylogeny reconstruction. Phylogenetic trees were reconstructed using the neighbor-joining algorithm (25) and the maximum-likelihood method. Neighbor-joining trees were obtained using MEGA, version 4 (33), with the maximum-composite-likelihood distance (34) in the case of nucleotide sequences and the Poisson correction for amino acid alignments (37). Support for the groupings derived in these reconstructions was evaluated by bootstrapping using 1,000 replicates (10). Maximum-likelihood trees were obtained using PhyML (13). The best evolutionary model for the sequences according to jModelTest (23) and considering the Akaike information criterion (AIC) turned out to be the generalized time-reversible model of substitution with a gamma distribution (GTR+G) accounting for heterogeneity in evolutionary rates among sites. This model was used to derive the maximum-likelihood trees obtained in this work. The whole or partial *rtxA1* genes of *V. cholerae* (strains M66-2, MO10, N16961, O395, and AM19226), *V. splendidus* (strain 12B01), *L. anguillarum* (strain M93), and *A. hydrophila* (strain ATCC 7966) were used as outgroups.

The congruence among phylogenetic reconstructions obtained with different alignments was checked using Shimodaira-Hasegawa (SH) (31) and expected-likelihood weight (ELW) tests as implemented in TreePuzzle, version 5.2 (29, 32).

A maximum-parsimony network using the Wagner method (9, 16) was constructed using the program MOVE in the PHYLIP package (PHYLIP, Phylogeny Inference Package, version 3.6[http://www.evolution.genetics.washington.edu]) from the presence/absence of the main domains in the *rtx* gene to show the relationships among the above genes.

Nucleotide sequence accession numbers. Sequences of the whole *rtxA1* genes determined in this study were deposited in the GenBank under accession numbers FJ002578 to FJ002581 and GU452642 to GU452644. Sequences of the common fragment of the *rtxA1* gene were deposited under accession numbers GU452542 to GU452641 and GU452645 to GU452660.

RESULTS

Location of the gene *rtxA1*. All *V. vulnificus* isolates tested of the three biotypes carried a copy of the *rtxA1* gene in the chromosome (described in the literature as chromosome II or "small chromosome" [7, 15]), and those of biotype 2 had an additional copy in the plasmid of 68 to 70 kb (see Fig. S1 in the supplemental material).

$MARTX_{Vv}$ toxin domain organization. Figure 1 shows the comparison of conserved and nonconserved domains of the predicted MARTX toxin for *V. vulnificus* (four sequences previously published and seven obtained in this work) compared with those of $MARTX_{Vc}$ toxin (strains M66-2, AM19226, MO10, O395, and N16961), $MARTX_{La}$ toxin (*L. anguillarum*) (strain M93), $MARTX_{Vs}$ toxin (strain 12B01), and the MARTX toxin of *A. hydrophila* ($MARTX_{Ah}$) (strain ATCC 7966). Tables 3 and 4 summarize the main structural characteristics of these proteins in *V. vulnificus*. The predicted proteins vary in length, ranging from 4,596 aa for biotype 2 isolates to 5,207 aa for three biotype 1 isolates (Fig. 1). The multiple alignment of $MARTX_{Vv}$ toxins showed that they could be divided in three regions, two corresponding to conserved sequences among biotypes, located at the N- and C-terminal ends, respectively, and another of variable sequence, located in the central portion of the protein (Fig. 1).

Within $MARTX_{Vv}$ toxin, the N- and C-terminal ends were very similar (93 to 100% and 90.5 to 100%, respectively) (see Table S1 in the supplemental material). The similarity of $MARTX_{Vv}$ toxin to the $MARTX_{Vc}$, $MARTX_{Vs}$, and $MARTX_{La}$ toxins was also high (61.1 to 100%) (with the exception of the strain O395, which lacks nearly all of the N-terminal region although similarity was even lower with $MARTX_{Ah}$ toxin [46.5 to 57.2%]) (see Table S1 in the supplemental material). According to Satchel (27), the MARTX

TABLE 2. Primer pairs for sequencing *rtxA1* in various strains

CECT 4999 (C), A14 (P), and 95-8-161 (P)[a]		CECT 529[T]		11028		94-9-119		Riu-1	
Primer	Sequence (5′–3′)	Primer	Sequence (5′–3′)	Primer	Sequence (5′–3′)	Primer	Sequence (5′–3′)	Primer	Sequence (5′–3′)
0F	GTGACGCTCTTTGGTGCTC	0F	GTGACGCTCTTTGGTGCTC	0F	GTGACGCTCTTTGGTGCTC	0F	GTGACGCTCTTTGGTGCTC	0F	GTGACGCTCTTTGGTGCTC
0R	CAGTCGTTTGTCTTTGGTG	0R	CAGTCGTTTGTCTTTGGTG	0R	CAGTCGTTTGTCTTTGGTG	0R	CAGTCGTTTGTCTTTGGTG	0R	CAGTCGTTTGTCTTTGGTG
1F	CCACACGGTTGAAGTTGCCA	1F	CCACACGGTTGAAGTTGCCA	1F	CCACACGGTTGAAGTTGCCA	1F	CCACACGGTTGAAGTTGCCA	1F	CCACACGGTTGAAGTTGCCA
1R	ACGCCAGAAGATTTGCCTCGT	1R	ACGCCAGAAGATTTGCCTCGT	1R	ACGCCAGAAGATTTGCCTCGT	1R	ACGCCAGAAGATTTGCCTCGT	1R	ACGCCAGAAGATTTGCCTCGT
2F	GACGAGGCAAATCTTCTGGCG	2F	GACGAGGCAAATCTTCTGGCG	2F	GACGAGGCAAATCTTCTGGCG	2F	GACGAGGCAAATCTTCTGGCG	2F	GACGAGGCAAATCTTCTGGCG
2R	GATGGATGCGAATGGTCTT	2R	GATGGATGCGAATGGTCTT	2R	GATGGATGCGAATGGTCTT	2R	GATGGATGCGAATGGTCTT	2R	GATGGATGCGAATGGTCTT
3F_Bt2	CGTCTACAGCCAGTTCAG	3F_Bt1	GATGTCGCCTTCCGCAATACC	3F_Bt1	GATGTCGCCTTCCGCAATACC	3F_Bt1	GATGTCGCCTTCCGCAATACC	3F_Bt2	CGTCTACAGCCAGTTCAG
3R_Bt2	GGTGGATGCGAAAGCGACT	3R_Bt2	GGTGGATGCGAAAGCGACT	5R_Bt1	CTGAGCAATCCAACCCTTTAC	3R_Bt1	GGAGTCACAGTCATTGGC	3R_Bt2	GGTGGATGCGAAAGCGACT
4F_Bt2	CTGTCTGAGTAAAGCGTTGG	4F_Bt2	CTGTCTGAGTAAAGCGTTGG	6F_Bt1	CCTGCCACACTTTCATC	4F2_Bt1	AATGTTGTTCGCAGCACCAG	4F_Bt2	CTGTCTGAGTAAAGCGTTGG
4R_Bt2	CAACCTGCGTGGCTATGG	6R_Bt1	GCGGTGTCTGGCTTATT	6R_Bt1	GCGGTGTCTGGCTTATT	4R2_Bt1	CAGGGCGTAATCAAGCG	4R_Bt2	CAACCTGCGTGGCTATGG
5F_Bt2	CGCTTTGGTCATACTTGGC	7F_Bt1	CGTTAGCAGCAGAATCGGCGT	7F_Bt1	CGTTAGCAGCAGAATCGGCGT	5F_Bt1	CGCATCAAAACCAAGGTCAC	5F_Riu1	CGGTCAAGCAATAAGCCAGA
5R_Bt2	ATGCGAAGAACCCAATG	7R_Bt1	TCTGAAGGCTATGCGAG	7R_Bt1	TCTGAAGGCTATGCGAG	5R_Bt1	CTGAGCAATCCAACCCTTTAC	5R_Riu1	GTATCTGGACGGAAACGG
6F_Bt2	GGTATCAAGAACATCAGTG	8F_Bt1	CTTCATCTGCTTGGCTGGC	6F_Riu1	GACAAGGCATCAAGGAG	6F_Bt1	CCTGCCACACTTTCATC	6F_Riu1	GACAAGGCATCAAGGAG
6R_Bt2	TGCTCGTCTCATTGCTTTC	8R_Bt1	GGATAACAAGGTGCTCTCGC	8R_Bt1	GGATAACAAGGTGCTCTCGC	6R_Bt1	GCGGTGTCTGGCTTATT	8F_Bt1	CTTCATCTGCTTGGCTGGC
7F_Bt2	GTCTTCCTGTAGTCCTTTC	8F1_Bt1	GATACTCCGTCAGGGCGT	8F1_Bt1	GATACTCCGTCAGGGCGT	7F_Bt1	CGTTAGCAGCAGAATCGGCGT	6R_Riu1	GTGGTATGTTCCTTGAC
7R_Bt2	CCAGTCAAACCACCAAAGC	8R1_Bt1	CGATTATGACTGGGACAAACGC	8R1_Bt1	CGATTATGACTGGGACAAACGC	7R_Bt1	TCTGAAGGCTATGCGAG	6R2_Riu1	GCTGGTGGTTTGTTAGA
8F_Bt2	GCCCATCATCACTCACC	8F2_Bt1	CCAGACCAGAAGGAAACAATGC	8F2_Bt1	CCAGACCAGAAGGAAACAATGC	8F_Bt1	CTTCATCTGCTTGGCTGGC	9F	GTGTGCGTCAGATTCGG
8R_Bt2	GTCCGTTGCGAAGTCTGAAGC	8R2_Bt1	GAAATCTGAAGCGGGTGTGG	8R2_Bt1	GAAATCTGAAGCGGGTGTGG	8R_Bt1	GGATAACAAGGTGCTCTCGC	9R	GAAGAAGTGGGCTCGGAC
9F	GTGTGCGTCAGATTCGG	9F	GTGTGCGTCAGATTCGG	9F	GTGTGCGTCAGATTCGG	8F1_Bt1	GATACTCCGTCAGGGCGT	10F	CCTTCACCATTCACGCCATA
9R	GAAGAAGTGGGCTCGGAC	9R	GAAGAAGTGGGCTCGGAC	9R	GAAGAAGTGGGCTCGGAC	8R1_Bt1	CGATTATGACTGGGACAACGC	10R	GGTGTTGTGGCGGCAGC
10F	CCTTCACCATTCACGCCATA	10F	CCTTCACCATTCACGCCATA	10F	CCTTCACCATTCACGCCATA	8F2_Bt1	CCAGACCAGAAGGAAACAATGC	11F	CAACAACCCTACCGTGG
10R	GGTGTTGTGGCGGCAGC	10R	GGTGTTGTGGCGGCAGC	10R	GGTGTTGTGGCGGCAGC	8R2_Bt1	GAAATCTGAAGCGGGTGTGG	11R	CCGCAGGTATGTTGGGC
11F	CAACAACCCTACCGTGG	11F	CAACAACCCTACCGTGG	11F	CAACAACCCTACCGTGG	9F	GTGTGCGTCAGATTCGG	12F	CACCGCCCATCACCGCAA
11R	CCGCAGGTATGTTGGGC	11R	CCGCAGGTATGTTGGGC	11R	CCGCAGGTATGTTGGGC	9R	GAAGAAGTGGGCTCGGAC	12R	AGTGTGCCATTGCCGTAGG
12F	CACCGCCCATCACCGCAA	12F	CACCGCCCATCACCGCAA	12F	CACCGCCCATCACCGCAA	10F	CCTTCACCATTCACGCCATA	13F	CACCGCTTGAACATCG
12R	CCTACGGCAATGGCACACT	12R	CCTACGGCAATGGCACACT	12R	CCTACGGCAATGGCACACT	10R	GGTGTTGTGGCGGCAGC	13R	AAGTGGCGATGGCAATGTG
13F	CACCGCTTGAACATCG	13F	CACCGCTTGAACATCG	13F	CACCGCTTGAACATCG	11F	CAACAACCCTACCGTGG	14F	CCTTGGTTGGTTTCAT
13R	AAGTGGCGATGGCAATGTG	13R	AAGTGGCGATGGCAATGTG	13R	AAGTGGCGATGGCAATGTG	11R	CCGCAGGTATGTTGGGC	14R	CTACTACGAAGATGAGCAC

14F	CCTTGGTTGGTTTCAT	14F	CCTTGGTTGGTTTCAT	14F	CCTTGGTTGGTTTCAT	12F	CACCGCCCATCACC		
							GCAA		
14R	CTACTACGAAGATGA	14R	CTACTACGAAGATGA	14R	CTACTACGAAGATGA	12R	CCTACGGCAATGGCA		
	GCAC		GCAC		GCAC		CACT		
						13F	CACCGCTTGAACATCG		
						13R	AAGTGGCGATGGCAA		
							TGTG		
						14F	CCTTGGTTGGTTTCAT		
						14R	CTACTACGAAGATGA		
							GCAC		

[a] C, *rtxA1* copy located on a chromosome; P, *rtxA1* copy located on a plasmid.

toxin subfamily carries three different types of repetitive sequences in the N- and C-terminal ends, which share a G-7X-GXXN central motif. We were unable to find these repeats in the same number and positions described by Satchell (27) in the strains we analyzed, which showed the following repetitive sequences: A-type repeat, GXXGXXXXXG; B-type repeat B.1, TXVGXGXX; B-type repeat B.2, GXANXXTXX; and C-type repeat, GGXGXDXXX. The results obtained for the redefined repeat sequences are shown in Table 3 and Fig. 1. The new repeats, their positions as well as the entire N and C termini, were highly conserved across the species and even within the genus (Fig. 1; see also Tables S2 to S5 in the supplemental material).

The internal region of the $MARTX_{Vv}$ toxin was very variable, showing a global identity and similarity of 18% and 44.5%, respectively (see Table S1). However, these values rose to over 95% for the group formed by the human biotype 1 isolates (YJ016, CMCP6, and 94-9-119) and to 100% for biotype 2 isolates (see Table S1).

The functional domains and their positions are presented in Fig. 1 and Table 4. Three different modular types of $MARTX_{Vv}$ toxins (called types I, II, and III) (Fig. 1) were found, all of which possessed a CPD domain, an α/β-hydrolase domain, and a newly reassigned domain, denoted Efa/LifA (common domains). This new domain corresponds to Mcf-DUF (27) and was renamed because of its very high similarity to the Efa/LifA-like protein of *Escherichia coli* O127:H6 E2348/69 (YP_002328637.1) (E-values between $2e^{-64}$ and $3e^{-65}$ for the domains of the different $MARTX_{Vv}$ toxins). $MARTX_{Vv}$ toxin type I was similar to the $MARTX_{Vvbt1}$ toxin described by Satchell (27). This type was present in human isolates of biotype 1, strains YJ016, CMCP6, and 94-9-119, and contained the common domains plus a DUF domain, with no similarity to any known protein (*V. vulnificus* DUF [DUF_{Vv}]), a RID domain, and a newly reassigned domain called *rtxA* of *Photorhabdus asymbiotica* ($rtxA_{PA}$). This new domain corresponds to PMT C1/C2 (27) and was renamed because of its similarity to the *rtxA* protein of *P. asymbiotica* (access number YP_003040934.1) (E-values of $3e^{-158}$ to $1e^{-170}$ for the domains of the different $MARTX_{Vv}$ toxins). $MARTX_{Vv}$ toxin type II was represented by the type strain of the species, isolate CECT 529^T of biotype 1, an environmental isolate of biotype 1, Riu-1, and the isolate of biotype 3, 11028. Type II differed from type I in that it lacked the $rtxA_{PA}$ domain, and, consequently, it was smaller (around 4,704 aa). $MARTX_{Vv}$ toxin type III was identical to $MARTX_{Vvbt2}$ toxin, a plasmidic variant described by Lee et al. (18), which, in addition to the common domains, had an ACD domain and two copies of the Efa/LifA domain flanking the common α/β-hydrolase domain.

$MARTX_{Vc}$ toxin of the five strains analyzed showed the same domain organization although $MARTX_{Vc}$ toxin of strain O395 lacked around 1,910 aa in the N-terminal region (Fig. 1). $MARTX_{La}$ toxin showed an organization similar to that of $MARTX_{Vv}$ toxin type II except that it lacked the DUF_{Vv} domain, and $MARTX_{Vs}$ toxin showed an organization similar to that of $MARTX_{Ah}$ toxin and different from that of the $MARTX_{Vv}$ and $MARTX_{Vc}$ toxins with a replacement of the ACD domain by a domain of unknown function different from that of *V. vulnificus* (*V. splendidus* DUF [DUF_{Vs}]).

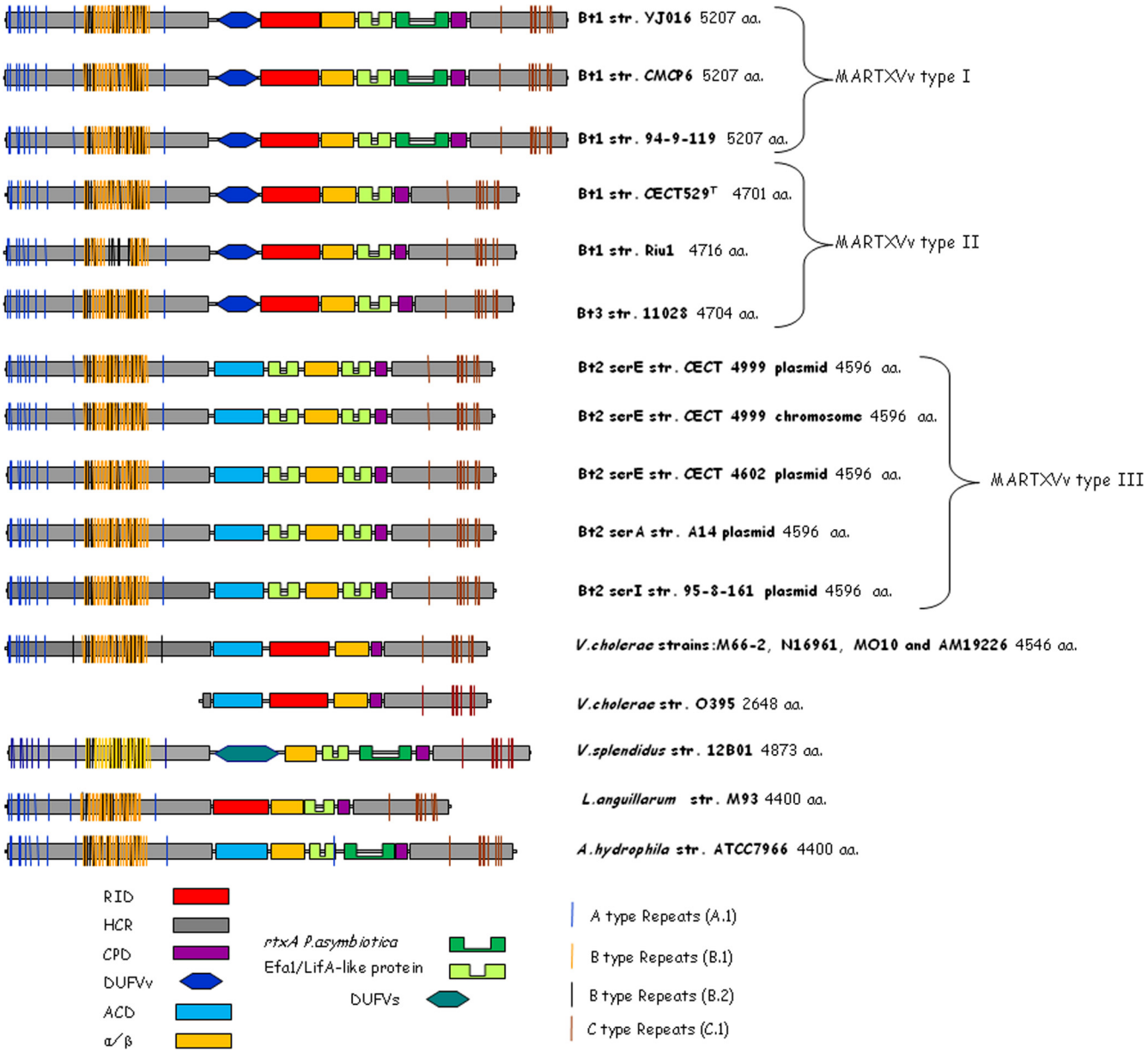

FIG. 1. Domain organization of the MARTX toxin structures from the analyzed genomes. The external regions, the repeats (vertical lines), and the internal domains for each toxin are color coded as indicated at the bottom of the figure. Diagrams are drawn to scale.

Phylogenetic reconstruction. The different phylogenetic trees derived from the complete nucleotide sequences from *V. vulnificus* and the outgroup species were coincident in revealing a topology in which *V. cholerae* strains formed a well-supported, monophyletic group quite distinct from its sister group, which included *V. vulnificus* and two other outgroups, *V. splendidus* and *L. anguillarum*, which were associated with *V. vulnificus* strain Riu-1 (Fig. 2). As a result of the variable patterns of modular organization among the different strains and species analyzed (Fig. 1), the phylogenetic reconstruction derived from the multiple alignment of the complete gene may not be an accurate representation of the evolutionary relationships among the different sequences considered. In fact, it was not possible to obtain a reliable alignment including the outgroup species *A. hydrophila*. Hence, alternative strategies were used to decipher the evolutionary history of *rtxA1* in these taxa. To this end, the phylogenetic trees from the external and internal regions of *rtxA1* were analyzed separately. As can be seen in Fig. 3, they were not congruent with one another or with the sequence from the whole gene (Fig. 2 and 3). Thus, all *V. vulnificus* isolates grouped together with *L. anguillarum* and separately from *V. cholerae* and *V. splendidus* when only the external 5′-terminal regions were considered (Fig. 3A); they formed a well-supported monophyletic group highly related to the *V. cholerae* group, with *V. splendidus* and *L. anguillarum* occupying external positions, when only the external 3′-terminal regions were considered. In contrast, *V. vulnificus* strains were divided into two groups, one formed by biotype 1 and 3

TABLE 3. Repeat sequences in $MARTX_{Vv}$ toxins

Strain (location of *rtxA1* gene copy)[a]	Profile of repeat sequences by type							
	A type A.1		B type B.1		B type B.2		C type C.1	
	No. of repeats	Location (aa)	No. of repeats	Location (aa)	No. of repeats	Location (aa)	No. of repeats	Location (aa)
V. vulnificus								
YJ016	9	30–1483	29	729–1330	18	742–1287	9	4584–5063
CECT 529^T	9	30–1480	29	726–1328	18	739–1284	9	4078–4557
Riu-1	9	30–1483	30	724–1325	18	756–1301	9	4096–4572
CMCP6	9	30–1483	29	729–1330	18	742–1287	9	4584–5063
94-9-119	9	30–1483	29	729–1330	18	742–1287	9	4584–5063
A14 (P)	9	30–1485	29	731–1332	18	744–1289	9	3973–4452
95-8-161 (P)	9	30–1485	29	731–1332	18	744–1289	9	3973–4452
CECT 4999 (C)	9	30–1485	29	731–1332	18	744–1289	9	3973–4452
CECT 4602 (P)	9	30–1485	29	731–1332	18	744–1289	9	3973–4452
CECT 4999 (P)	9	30–1485	29	731–1332	18	744–1289	9	3973–4452
11028	9	30–1483	29	729–1330	18	742–1287	9	4081–4560
V. cholerae M66-2	9	30–1478	29	726–1328	18	739–1284	9	3923–4402
A. hydrophila ATCC 7966	10	30–3012	27	704–1286	17	717–1224	9	4072–4542
L. anguillarum M93	9	30–1483	29	729–1330	18	742–1287	9	3783–4256

[a] C, chromosome; P, plasmid.

isolates together with *L. anguillarum* and *V. splendidus* as a basal taxon to this group and the other formed by biotype 2 isolates when only the internal region was considered (Fig. 3C). The phylogenetic reconstruction from the common fragment of 828 nt corresponding to the 5′ end of the *rtxA1* gene is shown in Fig. S2 in the supplemental material. The fragment was highly similar (95 to 100%) although there were differences between strains that were not related to biotype, with isolate Riu-1 presenting the largest number of substitutions (see Fig. S2). Nevertheless, the similarity between fragments was too high to infer any conclusive results from the evolutionary history of this portion of the gene.

A maximum-parsimony network showing the relationships among the genes from the presence/absence of the domains in the *rtxA1* gene is shown in Fig. 4. In this analysis, we included *A. hydrophila*, which was too divergent at the sequence level of the complete gene to be incorporated in the previous maximum-likelihood tree, and excluded *V. splendidus* because of its different modular organization (Fig. 1). The network suggested a very plastic modular organization in this gene, with a minimum of seven independent gains/losses of domains. Of these, only one homoplasy (the independent gain of domain $rtxA_{PA}$ in *A. hydrophila* and three strains of biotype 1) was found. Furthermore, *V. vulnificus* represented the most divergent gene organizations (with four or five gains/losses of domains) among the sequences included in the analysis.

The next issue we pursued was an individual analysis of each of these domains, for which we used the corresponding multiple nucleotide sequence alignments (Fig. 3D). The only domains common to all the strains and species considered were the α/β-hydrolase and CPD, and their phylogenetic histories were not congruent, again, to one another or with that derived with the complete sequences for this gene (Fig. 2 and 3). The most relevant discrepancies were for the α/β-hydrolase domain, for which the sequence from Riu-1 was identical to sequences from biotype 2 strains, and for the CPD domain, for which the three biotype 1 strains 94-9-119, CMCP6, and YJ016 grouped externally to the rest with *V. splendidus*, placing *V. cholerae* and *L. anguillarum* as members of the ingroup (Fig. 3D). The differences found among biotype 1 sequences for the α/β-hydrolase domain could be explained by an HGT event of this domain from one biotype 2 strain to Riu-1. The simplest explanation for the placement of the three biotype 1 sequences in the CPD domain phylogenetic tree is also their acquisition from an unidentified donor by an HGT event. To further verify these hypotheses, we performed reciprocal tests of congruence for the α/β-hydrolase and CPD domains and the complete gene sequences using the 13 strains common to all three data sets. The results of the Shimodaira-Hasegawa (SH) and expected-likelihood weight (ELW) tests are summarized in Table 5. All the comparisons were highly significant for both tests with only one exception, corresponding to the results of the SH test of the topology obtained with the complete gene sequences versus the CPD domain alignment and its maximum-likelihood tree. This indicates that the phylogenetic reconstructions obtained from each alignment were not congruent with one another, thus providing statistical support for the HGT hypothesis for both domains.

The remaining domains considered in this gene had a less constant distribution in the different strains and species considered. Biotype 2 strains presented two copies of the Efa1/LifA-like domain. The phylogenetic tree derived for the sequences in this domain suggests that the duplication probably occurred before the divergence of biotype 2 strains (Fig. 3D). This was not the only salient feature in the evolution of this domain. Here, the biotype 3 sequence (from strain 11028) grouped with one of the paralogous copies from biotype 2, the one that was not present in biotype 1 strains. Furthermore, two biotype 1 strains (CECT 529^T and 94-9-119) did not group with the remaining sequences from this biotype and diverged closer to the root of the *V. vulnificus* group than they did in the maximum-likelihood tree for the whole-gene alignment. Interestingly, one outgroup sequence, corresponding to *L. anguillarum*, was very similar to, and grouped with, sequences from *V. vulnificus* biotype 1 strains. This resem-

TABLE 4. Putative functional domains in $MARTX_{Vv}$ toxins

Strain (location of *rtxA1* gene copy)[a]	Domain name[b]	Protein		Gene	
		Position (aa)	% Identity[c]	Position (aa)	% Identity[c]
YJ016	DUF	1957–2345	ND	5871–7035	ND
	RID	2368–2915	87.6	7081–8719	82.4
	α/β-Hydrolase	2918–3277	85.8	8709–9609	89.7
	Efa1/LifA	3276–3519	54.1	9844–10569	55.5
	$rtxA_{PA}$	3604–4080	57	10789–12201	61.4
	CPD	4082–4188	75.7	12202–12525	70.6
CMCP6	DUF	1957–2345	ND	5871–7035	ND
	RID	2368–2915	87.6	7081–8719	82.2
	α/β-Hydrolase	2918–3277	85.8	8709–9609	89.1
	Efa1/LifA	3276–3519	54.1	9844–10569	55.6
	$rtxA_{PA}$	3604–4080	57	10789–12201	61.5
	CPD	4082–4188	75.7	12202–12525	70
94-9-119	DUF	1957–2345	ND	5871–7035	ND
	RID	2368–2915	86.5	7081–8719	81.1
	α/β-Hydrolase	2918–3277	85.2	8709–9609	89.5
	Efa1/LifA	3276–3519	53.4	9844–10569	55.6
	$rtxA_{PA}$	3604–4080	57	10789–12201	61.4
	CPD	4082–4188	76.6	12202–12525	70.3
CECT 529^T	DUF	1954–2342	ND	5862–7026	ND
	RID	2365–2912	86.3	7072–8710	80,9
	α/β-Hydrolase	2915–3224	86.1	8700–9600	89.6
	Efa1/LifA	3273–3516	53.4	9839–10548	56.2
	CPD	3576–3682	86.9	10687–11007	75.5
Riu-1	DUF	1971–2359	ND	5913–7077	ND
	RID	2382–2929	80.1	7123–8761	78.9
	α/β-Hydrolase	2932–3241	86.8	8751–9651	90
	Efa1/LifA	3290–3533	54.3	9870–10599	57.0
	CPD	3593–3699	86	10738–11058	75.8
CECT 4999 (C)	ACD	1958–2421	89	5856–7225	82.5
CECT 4999 (P)	Efa1/LifA (copy 1)	2492–2735	53.9	7495–8205	56.7
CECT 4602 (P)	α/β-Hydrolase	2810–3119	86.5	8385–9285	97.1
A14 (P)	Efa1/LifA (copy 2)	3168–3411	54.3	9523–10233	56.7
94-9-161 (P)	CPD	3471–3577	86	10372–10692	76.1
11028	DUF	1957–2345	ND	5871–7035	ND
	RID	2368–2915	83.6	7081–8719	81.5
	α/β-Hydrolase	2918–3227	86.1	8709–9609	90.2
	Efa1/LifA	3276–3519	53.9	9844–10569	56.3
	CPD	3579–3685	86	10695–11016	76.1

[a] C, chromosome; P, plasmid.
[b] CPD, autocatalytic cysteine protease domain; Efa/LifA, LifA-like protein of *Escherichia coli* O127:H6 E2348/69; RID, Rho-GTPase inactivation domain; DUF_{Vv}, domain with an unknown function; rtx_{PA}, *rtxA* of *P. asymbiotica*; ACD, actin cross-linking domain.
[c] Percent identity with the *V. cholerae* N16961 *rtxA* gene for ACD, RID, CPD, and α/β-hydrolase domains, with the *E. coli* Efa/LifA gene for the Efa1/LifA domain, and with the *P. asymbiotica rtxA* gene for $rtxA_{PA}$ domain. ND, no similarity detected.

blance was also revealed in the previous analysis of the distribution of domains (Fig. 4) and by the phylogenetic tree from the internal part of the gene (Fig. 3C).

Domains ACD, DUF_{Vv}, RID, and $rtxA_{PA}$ were present in only a few strains (Fig. 3D), and their corresponding phylogenetic trees were not too informative on the evolution of the *rtxA1* gene. ACD was present in only biotype 2 strains and in the outgroups *V. cholerae* and *A. hydrophila*, whereas RID was present in biotype 1 and 3 strains and in the outgroups *V. cholerae* and *L. anguillarum* (Fig. 1 and 3D). In both cases, the within-biotype distribution of evolutionary distances was very similar to that observed in the analysis of the complete gene (Fig. 2). Domain $rtxA_{PA}$ was present in only three biotype 1 strains and in three outgroups (*P. asymbiotica*, *V. splendidus*, and *A. hydrophila*) but not in *V. cholerae*. Finally, DUF_{Vv} was present in only *V. vulnificus* biotypes 1 and 3. In fact, this domain did not show similarity to known proteins by BLAST search. Similar to other portions in this gene, the strain Riu-1 presented a remarkable accumulation of mutations in comparison to other strains of the same subtype.

DISCUSSION

In the first part of this work, we have analyzed the structural diversity of MARTX toxins in *V. vulnificus* biotypes by comparing them to other MARTX toxins. We have found three different modular types according to the domains identified in

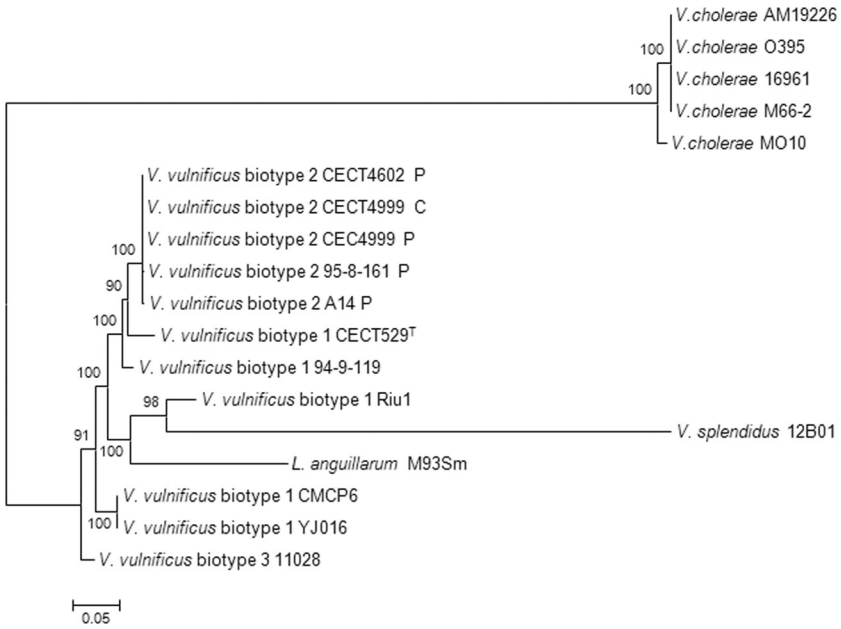

FIG. 2. Maximum-likelihood tree derived from the aligned regions from complete *rtxA1* gene sequences (20,394 nt) using the GTR+G model of evolution. Bootstrap support values higher than 80% are indicated in the corresponding nodes.

the internal part of the protein. In contrast, the external regions are highly conserved within the species and even the genus, which correlates with the proposed function for these regions, that is, to interact with the membrane of eukaryotic cells allowing the translocation of effector domains to the cytoplasm. Upon translocation, CPD is activated to process the MARTX toxin, thereby releasing the internal domains, which alter cell function (30). We have redefined two of the internal domains, Mcf-DUF and PMT C1/C2 (originally described by Satchell [27]) as Efa/LifA and rtx_{PA}, respectively, because of the new similarities revealed by BLAST searches. Lymphostatin (Efa/LifA protein) is a common toxin in Gram-negative bacteria with multiple functions, cell adhesion, immunosuppression, and disruption of epithelial barrier function via the modulation of Rho GTPase activities, while no function has been reported for the *rtxA* of *P. asymbiotya*. Biotype 1 isolates feature $MARTX_{Vv}$ toxin type I, a type already described by Satchell (27), and type II, which is simpler than the former because it lacks the rtx_{PA} domain. In addition, all *V. vulnificus* biotype 2 isolates, irrespective of their serovar, have $MARTX_{Vv}$ toxin type III described by Lee et al. (18) and harbor two copies of the gene, one plasmidic and the other chromosomal. It has been proposed that $MARTX_{Vv}$ toxin type I is the main factor for human virulence in *V. vulnificus* since mutations in this gene practically abolish virulence in mice (19). However, we have found that other human isolates (the biotype 3 isolate) can produce a different type of toxin that lacks the rtx_{PA} domain, which would suggest that this domain is not necessary for virulence. In addition, we have found that fish-pathogenic isolates (biotype 2) show a different type, which could be related to specific virulence for fish. The role of the new types of $MARTX_{Vv}$ toxins in virulence as well as the reason for gene duplication in the biotype 2 remains to be elucidated.

In the second part of this work, we have analyzed the *rtxA1* gene using different data sets demonstrating that $MARTX_{Vv}$ toxins are mosaics of segments with different evolutionary histories. Previous studies of the evolution of *V. vulnificus* based on sequence-based typing of housekeeping genes suggest that the species can be subdivided into two recent and rapidly expanding phylogenetic clusters (8). One lineage would correspond to biotype 1 isolates, mostly from human sources, including the strains YJO16 and CMCP6 used in this study. The other lineage would be formed by biotype 1 and 2 isolates from various environments, including diseased fish. The phylogenetic position of biotype 3 isolates, which are genetically identical, would be variable depending on the gene and the model and method of analysis (6). An ongoing phylogenetic study of in lab using sequence-based typing of housekeeping and virulence-related genes (26) with the same strains included in the present work suggests that *V. vulnificus* species are subdivided in three lineages, one including biotype 1 and 2 from the fish farming environment, another including biotype 3 isolates, and a third including biotype 1 strains from human blood and the environment. Interestingly, none of the evolutionary histories inferred from the *rtxA1* gene matched the previously hypothesized evolutionary histories of *V. vulnificus* (6, 8, 26). The phylogenetic tree derived from the complete *rtxA1* gene (Fig. 2) presented an unlikely evolutionary scenario: *V. cholerae* isolates conformed to a well-supported, monophyletic group, but this was not the case for *V. vulnificus*, which included two outgroups, *V. splendidus* and *L. anguillarum*, both related to strain Riu-1. The inclusion of outgroup species within the ingroup can be due to several reasons, which we tried to analyze next by dividing the gene in three different portions. These fragments showed very different evolutionary relationships, which also differed from the previous result with the complete gene. The 5′ end (Fig. 3A) and the internal portion (Fig. 3C)

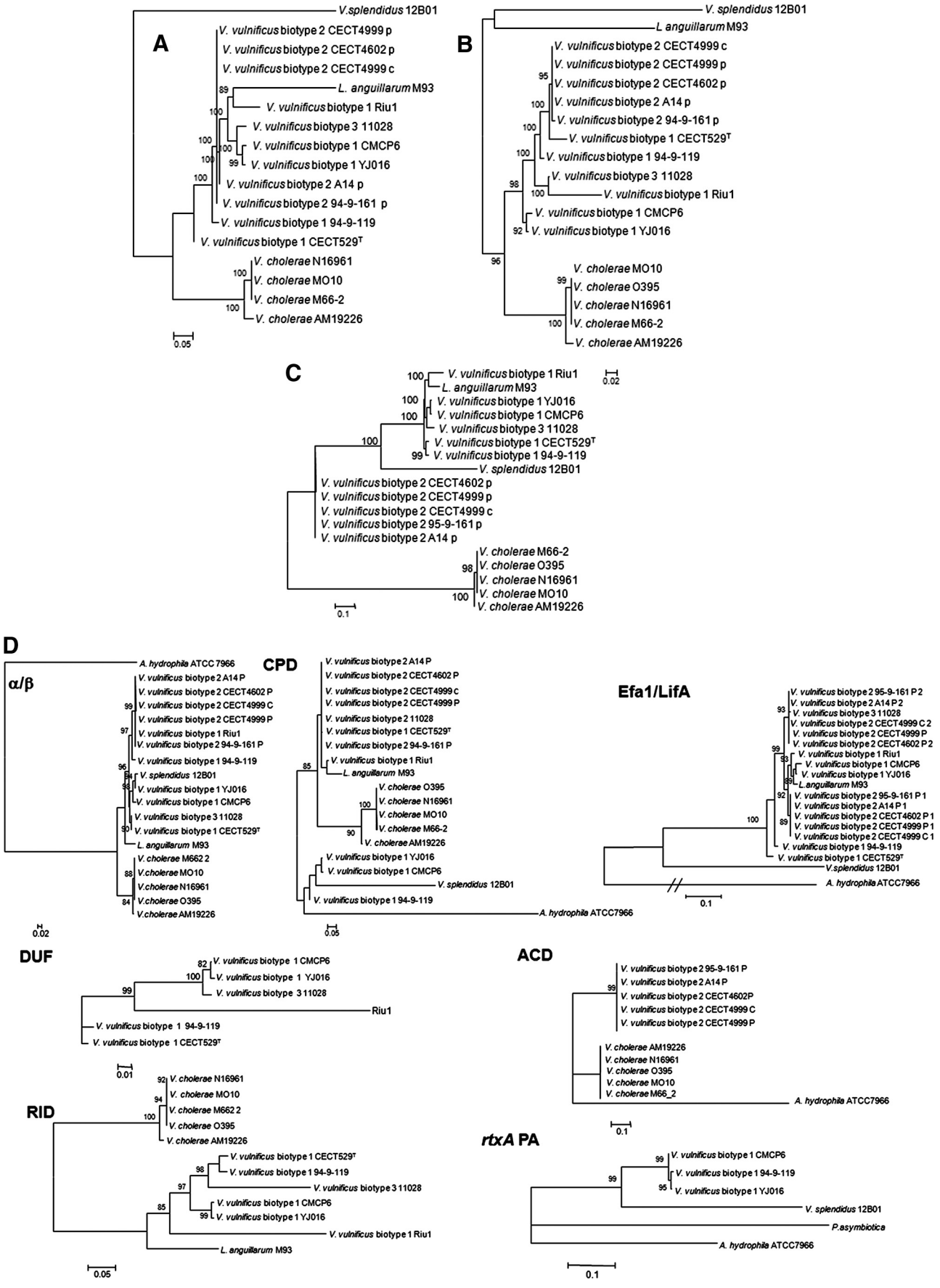
A
V.splendidus 12B01
V. vulnificus biotype 2 CECT4999 p
V. vulnificus biotype 2 CECT4602 p
V. vulnificus biotype 2 CECT4999 c
L. anguillarum M93
V. vulnificus biotype 1 Riu1
V. vulnificus biotype 3 11028
V. vulnificus biotype 1 CMCP6
V. vulnificus biotype 1 YJ016
V. vulnificus biotype 2 A14 p
V. vulnificus biotype 2 94-9-161 p
V. vulnificus biotype 1 94-9-119
V. vulnificus biotype 1 CECT529T
V. cholerae N16961
V. cholerae MO10
V. cholerae M66-2
V. cholerae AM19226
0.05
B
V. splendidus 12B01
L. anguillarum M93
V. vulnificus biotype 2 CECT4999 c
V. vulnificus biotype 2 CECT4999 p
V. vulnificus biotype 2 CECT4602 p
V. vulnificus biotype 2 A14 p
V. vulnificus biotype 2 94-9-161 p
V. vulnificus biotype 1 CECT529T
V. vulnificus biotype 1 94-9-119
V. vulnificus biotype 3 11028
V. vulnificus biotype 1 Riu1
V. vulnificus biotype 1 CMCP6
V. vulnificus biotype 1 YJ016
V. cholerae MO10
V. cholerae O395
V. cholerae N16961
V. cholerae M66-2
V. cholerae AM19226
C
V. vulnificus biotype 1 Riu1
L. anguillarum M93
V. vulnificus biotype 1 YJ016
V. vulnificus biotype 1 CMCP6
V. vulnificus biotype 3 11028
V. vulnificus biotype 1 CECT529T
V. vulnificus biotype 1 94-9-119
V. splendidus 12B01
V. vulnificus biotype 2 CECT4602 p
V. vulnificus biotype 2 CECT4999 p
V. vulnificus biotype 2 CECT4999 c
V. vulnificus biotype 2 95-9-161 p
V. vulnificus biotype 2 A14 p
V. cholerae M66-2
V. cholerae O395
V. cholerae N16961
V. cholerae MO10
V. cholerae AM19226
0.02
0.1
D
α/β
A. hydrophila ATCC 7966
V. vulnificus biotype 2 A14 P
V. vulnificus biotype 2 CECT4602 P
V. vulnificus biotype 2 CECT4999 C
V. vulnificus biotype 2 CECT4999 P
V. vulnificus biotype 1 Riu1
V. vulnificus biotype 2 94-9-161 P
V. vulnificus biotype 1 94-9-119
V. splendidus 12B01
V. vulnificus biotype 1 YJ016
V. vulnificus biotype 1 CMCP6
V. vulnificus biotype 3 11028
V. vulnificus biotype 1 CECT529T
L. anguillarum M93
V. cholerae M662 2
V.cholerae MO10
V.cholerae N16961
V.cholerae O395
V.cholerae AM19226
0.02
CPD
V. vulnificus biotype 2 A14 P
V. vulnificus biotype 2 CECT4602 P
V. vulnificus biotype 2 CECT4999 C
V. vulnificus biotype 2 CECT4999 P
V. vulnificus biotype 2 11028
V. vulnificus biotype 1 CECT529T
V. vulnificus biotype 2 94-9-161 P
V. vulnificus biotype 1 Riu1
L. anguillarum M93
V. cholerae O395
V. cholerae N16961
V. cholerae MO10
V. cholerae M66-2
V. cholerae AM19226
V. vulnificus biotype 1 YJ016
V. vulnificus biotype 1 CMCP6
V. splendidus 12B01
V. vulnificus biotype 1 94-9-119
A. hydrophila ATCC7966
0.05
Efa1/LifA
V. vulnificus biotype 2 95-9-161 P 2
V. vulnificus biotype 2 A14 P 2
V. vulnificus biotype 3 11028
V. vulnificus biotype 2 CECT4999 C 2
V. vulnificus biotype 2 CECT4999 P
V. vulnificus biotype 2 CECT4602 P 2
V. vulnificus biotype 1 Riu1
V. vulnificus biotype 1 CMCP6
V. vulnificus biotype 1 YJ016
L.anguillarum M93
V. vulnificus biotype 2 95-9-161 P 1
V. vulnificus biotype 2 A14 P 1
V. vulnificus biotype 2 CECT4602 P 1
V. vulnificus biotype 2 CECT4999 P 1
V. vulnificus biotype 2 CECT4999 C 1
V. vulnificus biotype 1 94-9-119
V. vulnificus biotype 1 CECT529T
V.splendidus 12B01
A. hydrophila ATCC7966
0.1
DUF
V. vulnificus biotype 1 CMCP6
V. vulnificus biotype 1 YJ016
V. vulnificus biotype 3 11028
Riu1
V. vulnificus biotype 1 94-9-119
V. vulnificus biotype 1 CECT529T
0.01
RID
V. cholerae N16961
V. cholerae MO10
V. cholerae M662 2
V. cholerae O395
V. cholerae AM19226
V. vulnificus biotype 1 CECT529T
V. vulnificus biotype 1 94-9-119
V. vulnificus biotype 3 11028
V. vulnificus biotype 1 CMCP6
V. vulnificus biotype 1 YJ016
V. vulnificus biotype 1 Riu1
L. anguillarum M93
0.05
ACD
V. vulnificus biotype 2 95-9-161 P
V. vulnificus biotype 2 A14 P
V. vulnificus biotype 2 CECT4602P
V. vulnificus biotype 2 CECT4999 C
V. vulnificus biotype 2 CECT4999 P
V. cholerae AM19226
V. cholerae N16961
V. cholerae O395
V. cholerae MO10
V. cholerae M66_2
A. hydrophila ATCC7966
0.1
rtxA PA
V. vulnificus biotype 1 CMCP6
V. vulnificus biotype 1 94-9-119
V. vulnificus biotype 1 YJ016
V. splendidus 12B01
P.asymbiotica
A. hydrophila ATCC7966
0.1

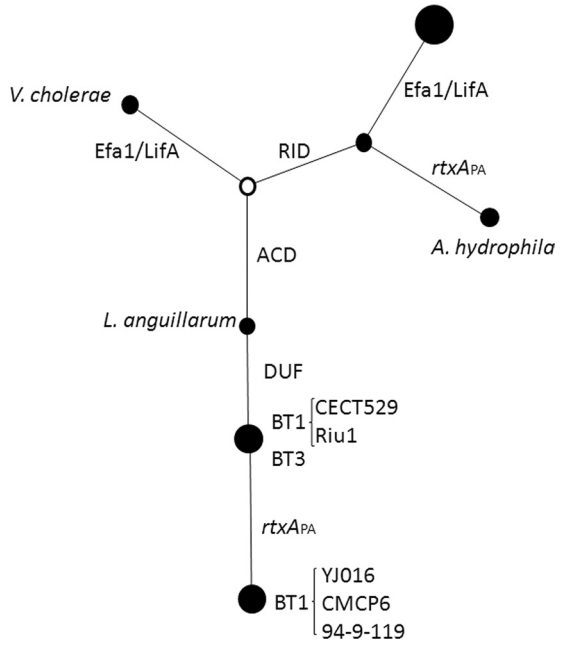

FIG. 4. Maximum-parsimony reconstruction of the presence/absence of modules in the central portion of *rtxA1* genes in the genomes analyzed. Gains or losses of domains are indicated next to each branch.

were partially coincident, but the placement of *V. splendidus* differed in the two trees, being an outgroup to all the sequences in the N-terminal coding portion of the gene and basal to a subgroup of *V. vulnificus* (including biotypes 1 and 3 and *L. anguillarum*) in the central portion. The 3′-end coding portion of the gene provided yet another history, but in this case the outgroup species appeared where they were supposed to (Fig. 3B). These results indicated that *rtxA1* of *V. vulnificus* has a complex evolutionary history, and this is also probably true for other closely related species. The modular structure of the gene may be partially responsible for this complexity (Fig. 1) and, in consequence, our next step was to investigate the evolutionary history of these modules.

The maximum-parsimony network for the module composition helped to disentangle the complex history of this protein (Fig. 4). The analysis of gains/losses of modules revealed that *V. vulnificus* biotype 2 isolates are closer to *A. hydrophila* than to the other biotypes of the species and that there have been several gain/loss events between biotype 2 and biotypes 1 and 3.

The most likely explanation for this complex evolutionary history involves HGT events from other bacteria and subsequent recombination, yielding new combinations, which might have been favored by selection. The *rtxA1* gene belongs to the segmentally variable gene family, previously defined as mosaics of one or more rapidly evolving, variable regions interrupted by conserved regions. Many of the mosaic genes identified encode proteins involved in host-pathogen interactions, defense mechanisms, and intracellular responses to external changes, and this is the case for $MARTX_{Vv}$ toxin. We have detected by the bioinformatic analysis evidence of at least two HGT events affecting the α/β-hydrolase and CPD domains and probably also to the Efa/LifA domain a fragment duplicated in biotype 2 isolates. In the cases of the α/β-hydrolase and Efa/LifA domains, the transferred DNA was probably from the same species, whereas in case of the CPD domain, it probably came from a different, unknown donor.

With regard to the domains ACD, DUF_{Vv}, RID, and $rtxA_{PA}$, we can suggest that (i) the DUF_{Vv} domain is exclusive of *V. vulnificus* biotype 1 and does not show similarity to known proteins, (ii) the $rtxA_{PA}$ domain of *V. vulnificus* is too different from *rtxA* of *P. asymbiotica* to have been received directly from this donor by HGT, and (iii) the ACD and RID domains have not been received from the species considered (*V. cholerae* or *V. cholerae*/*L. anguillarum*, respectively) because the distance for these domains is similar to that for the rest of the studied common domains. In the light of these results, the hypothesis of the origin of the ACD domain of $MARTX_{Vv}$ toxin type III from the ACD domain of $MARTX_{Vc}$ toxin has to be discarded.

V. vulnificus expresses a natural competence system induced by chitin (14) that has also been described in *V. cholerae* (21), which could work under natural conditions and favor the exchange of genetic material. In addition, the species possesses conjugative plasmids, which can be transmitted between strains and can even mobilize other resident plasmids (such as the virulence one) by forming cointegrates (18). Both genetic exchange mechanisms can result in coinfection with two different but related *rtx* genes, which could recombine, resulting in a new, different *rtx* gene. This process is exemplified in the biotype 2 of the species, which has a duplicated *rtxA1* gene in the chromosome and in the plasmid and produces a MARTX toxin that is completely different from the toxins of biotypes 1 and 3. The presence of identical duplicate genes in the genome of the biotype 2 isolates suggests that either the acquisition has been recent or a strong purifying selection is acting against mutations that modify gene function.

The phylogenetic study performed in our lab (26) demonstrates that biotype 2 is polyphyletic and suggests that it has emerged by acquisition of a virulence plasmid from *V. vulnificus* isolates from fish farms. According to this hypothesis, the acquisition of the plasmid could have occurred before or after divergence from the common ancestor for biotype 2 strains. The phylogenetic analysis shown here suggests that the duplication of the Efa/LifA domain likely occurred after the divergence between biotypes 1 and 2 and before the expansion of the biotype 2 clonal complex and, in consequence, more or less contemporaneously to the acquisition of the virulence plasmid mentioned above. This acquisition might have favored recombination events between the chromosomal and plasmidic *rtxA1* genes, and the selection of a new combination of the mosaic gene would probably have been advantageous in the

FIG. 3. Maximum-likelihood trees derived from 5′-terminal (A), 3′-terminal (B), and internal (C) regions of the *rtxA1* gene using the GTR+G model of evolution. The numbers of nucleotide positions considered in the multiple alignments were 5,844, 3,039, and 7,988, respectively. Bootstrap support values higher than 80% are indicated in the corresponding nodes. (D) Maximum-likelihood tree derived from the different modules of the *rtxA1* gene using the GTR+G model of evolution. Bootstrap support values higher than 80% are indicated in the corresponding nodes.

TABLE 5. Summary of SH and ELW tests for the complete *rtxA1* gene sequence and those obtained for the α/β-hydrolase and CPD modules using the 13 common strains and species[a]

Alignment	Topology	lnL	SH test	ELW test
Complete	Complete	−70351.24	1.000	1.000
	α/β-Hydrolase domain	−72657.44	0.000	0.000
	CPD domain	−76609.58	0.000	0.000
α/β-Hydrolase module	α/β-Hydrolase domain	−2165.08	1.000	1.000
	Complete	−2287.23	0.000	0.000
	CPD domain	−2235.99	0.000	0.000
CPD module	CPD domain	−1150.62	1.000	0.971
	Complete	−1159.13	0.273	0.029
	α/β-Hydrolase domain	−1252.89	0.000	0.000

[a] Each alignment was used to evaluate the log likelihood (lnL) of the ML tree obtained with each of the three data sets. The probability values for each topology and test are shown. Complete, complete *rtxA1* gene sequence.

fish farming environment and, in consequence, would have spread rapidly throughout suitable habitats throughout the seas, appearing as highly conserved among the different clonal complexes. The reasons for such an advantage will have to be elucidated by obtaining mutants deficient for the different domains and their combinations and then testing these mutants in selected *in vitro* models and *in vivo*.

ACKNOWLEDGMENTS

This work has been financed by grants AGL2008-03977/ACU and BFU2008-03000 and by Programa Consolider-Ingenio CSD2009-00006 from MICINN and project ACOMP/2009/240 from Conselleria d'Educació (Generalitat Valenciana).

We thank the SCSIE of the University of Valencia for technical support in determining the sequences.

REFERENCES

1. **Amaro, C., and E. G. Biosca.** 1996. *Vibrio vulnificus* biotype 2, pathogenic for eels, is also an opportunistic pathogen for humans. Appl. Environ. Microbiol. **62:**1454–1457.
2. **Amaro, C., E. G. Biosca, B. Fouz, and E. Garay.** 1992. Electrophoretic analysis of heterogeneous lipopolysaccharides from various strains of *Vibrio vulnificus* biotypes 1 and 2 by silver staining and immunoblotting. Curr. Microbiol. **25:**99–104.
3. **Ausubel, F. M., R. Brent, R. E. Kingston, D. D. Moore, J. G. Seidman, J. A. Smith, and K. Struhl.** 2007. Current protocols in molecular biology. John Wiley, New York, NY.
4. **Bisharat, N., V. Agmon, R. Finkelstein, R. Raz, G. Ben-Dror, L. Lerner, S. Soboh, R. Colodner, D. N. Cameron, D. L. Wykstra, D. L. Swerdlow, and J. J. Farmer III.** 1999. Clinical, epidemiological, and microbiological features of *Vibrio vulnificus* biogroup 3 causing outbreaks of wound infection and bacteraemia in Israel. Lancet **354:**1421–1424.
5. **Bisharat, N., C. Amaro, B. Fouz, A. Llorens, and D. I. Cohen.** 2007. Serological and molecular characteristics of *Vibrio vulnificus* biotype 3: evidence for high clonality. Microbiology **153:**846–856.
6. **Bisharat, N., D. I. Cohen, M. C. Maiden, D. W. Crook, T. Peto, and R. M. Harding.** 2007. The evolution of genetic structure in the marine pathogen, *Vibrio vulnificus*. Infect. Genet. Evol. **7:**685–693.
7. **Chen, C. Y., K. M. Wu, Y. C. Chang, C. H. Chang, H. C. Tsai, T. L. Liao, Y. M. Liu, H. J. Chen, A. B. Shen, J. C. Li, T. L. Su, C. P. Shao, C. T. Lee, L. I. Hor, and S. F. Tsai.** 2003. Comparative genome analysis of *Vibrio vulnificus*, a marine pathogen. Genome Res. **13:**2577–2587.
8. **Cohen, A. L., J. D. Oliver, A. DePaola, E. J. Feil, and E. F. Boyd.** 2007. Emergence of a virulent clade of *Vibrio vulnificus* and correlation with the presence of a 33-kilobase genomic island. Appl. Environ. Microbiol. **73:**5553–5565.
9. **Eck, R. V., and M. O. Dayhoff.** 1966. Evolution of the structure of ferredoxin based on living relics of primitive amino acid sequences. Science **152:**363–366.
10. **Felsenstein, J.** 1985. Confidence limits on phylogenies: an approach using the bootstrap. Evolution **39:**783–791.
11. **Fouz, B., F. J. Roig, and C. Amaro.** 2007. Phenotypic and genotypic characterization of a new fish-virulent *Vibrio vulnificus* serovar that lacks potential to infect humans. Microbiology **153:**1926–1934.
12. **Gasteiger, E., A. Gattiker, C. Hoogland, I. Ivanyi, R. D. Appel, and A. Bairoch.** 2003. ExPASy: the proteomics server for in-depth protein knowledge and analysis. Nucleic Acids Res. **31:**3784–3788.
13. **Guindon, S., and O. Gascuel.** 2003. A simple, fast, and accurate algorithm to estimate large phylogenies by maximum likelihood. Syst. Biol. **52:**696–704.
14. **Gulig, P. A., M. S. Tucker, P. C. Thiaville, J. L. Joseph, and R. N. Brown.** 2009. User friendly cloning coupled with chitin-based natural transformation enables rapid mutagenesis of *Vibrio vulnificus*. Appl. Environ. Microbiol. **75:**4936–4949.
15. **Kim, Y. R., S. E. Lee, C. M. Kim, S. Y. Kim, E. K. Shin, D. H. Shin, S. S. Chung, H. E. Choy, A. Progulske-Fox, J. D. Hillman, M. Handfield, and J. H. Rhee.** 2003. Characterization and pathogenic significance of *Vibrio vulnificus* antigens preferentially expressed in septicemic patients. Infect. Immun. **71:**5461–5471.
16. **Kluge, A. G., and J. S. Farris.** 1969. Quantitative phyletics and the evolution of anurans. Syst. Zool. **18:**1–32.
17. **Lee, B. C., S. H. Choi, and T. S. Kim.** 2008. *Vibrio vulnificus* RTX toxin plays an important role in the apoptotic death of human intestinal epithelial cells exposed to *Vibrio vulnificus*. Microbes Infect. **10:**1504–1513.
18. **Lee, C. T., C. Amaro, K. M. Wu, E. Valiente, Y. F. Chang, S. F. Tsai, C. H. Chang, and L. I. Hor.** 2008. A common virulence plasmid in biotype 2 *Vibrio vulnificus* and its dissemination aided by a conjugal plasmid. J. Bacteriol. **190:**1638–1648.
19. **Lee, J. H., M. W. Kim, B. S. Kim, S. M. Kim, B. C. Lee, T. S. Kim, and S. H. Choi.** 2007. Identification and characterization of the *Vibrio vulnificus* rtxA essential for cytotoxicity in vitro and virulence in mice. J. Microbiol. **45:**146–152.
20. **Li, L., J. L. Rock, and D. R. Nelson.** 2008. Identification and characterization of a repeat-in-toxin gene cluster in *Vibrio anguillarum*. Infect. Immun. **76:**2620–2632.
21. **Meibom, K. L., M. Blokesch, N. A. Dolganov, C. Y. Wu, and G. K. Schoolnik.** 2005. Chitin induces natural competence in *Vibrio cholerae*. Science **310:**1824–1827.
22. **Oliver, J. D.** 2006. *Vibrio vulnificus*, p. 349–366. *In* F. L. Thompson, B. Austin, and J. Swings (ed.), Biology of vibrios. ASM Press, Washington, DC.
23. **Posada, D.** 2008. jModelTest: phylogenetic model averaging. Mol. Biol. Evol. **25:**1253–1256.
24. **Roig, F. J., and C. Amaro.** 2009. Plasmid diversity in *Vibrio vulnificus* biotypes. Microbiology **155:**489–497.
25. **Saitou, N., and M. Nei.** 1987. The neighbor-joining method: a new method for reconstructing phylogenetic trees. Mol. Biol. Evol. **4:**406–425.
26. **Sanjuan, E., F. Gonzalez-Candelas, and C. Amaro.** 2011. Polyphyletic origin of *Vibrio vulnificus* biotype 2 as revealed by sequence-based analysis. Appl. Environ. Microbiol. **77:**688–695.
27. **Satchell, K. J. F.** 2007. MARTX, multifunctional autoprocessing repeats-in-toxin toxins. Infect. Immun. **75:**5079–5084.
28. **Satchell, K. J. F., and B. Geissler.** 2009. The multifunctional-autoprocessing RTX toxins of vibrios, p. 113–126. *In* Thomas Proft (ed.), Microbial toxins: current research and future trends. Caister Academic Press, Auckland, New Zealand.
29. **Schmidt, H. A., K. Strimmer, M. Vingron, and A. von Haeseler.** 2002. Tree-Puzzle: maximum likelihood phylogenetic analysis using quartets and parallel computing. Bioinformatics **18:**502–504.
30. **Sheahan, K. L., C. L. Cordero, and K. J. Satchell.** 2007. Autoprocessing of the *Vibrio cholerae* RTX toxin by the cysteine protease domain. EMBO J. **26:**2552–2561.
31. **Shimodaira, H., and M. Hasegawa.** 1999. Multiple comparisons of log-likelihoods with applications to phylogenetic inference. Mol. Biol. Evol. **16:**1114–1116.
32. **Strimmer, K., and A. Rambaut.** 2002. Inferring confidence sets of possibly misspecified gene trees. Proc. Biol. Sci. **269:**137–142.
33. **Tamura, K., J. Dudley, M. Nei, and S. Kumar.** 2007. MEGA4: molecular evolutionary genetics analysis (MEGA) software version 4.0. Mol. Biol. Evol. **24:**1596–1599.
34. **Tamura, K., M. Nei, and S. Kumar.** 2004. Prospects for inferring very large phylogenies by using the neighbor-joining method. Proc. Natl. Acad. Sci. U. S. A. **101:**11030–11035.
35. **Tison, D. L., M. Nishibuchi, J. D. Greenwood, and R. J. Seidler.** 1982. *Vibrio vulnificus* biogroup 2: new biogroup pathogenic for eels. Appl. Environ. Microbiol. **44:**640–646.
36. **Zhou, C., Y. Yang, and A. Y. Jong.** 1990. Mini-prep in ten minutes. Biotechniques **8:**172–173.
37. **Zuckerkandl, E., and L. Pauling.** 1965. Evolutionary divergence and convergence in proteins, p. 97–166. *In* V. Bryson and H. J. Vogel (ed.), Evolving genes and proteins. Academic Press, New York, NY.